

# In Vivo Airway Surface Liquid $\text{Cl}^-$ Analysis with Solid-state Electrodes

RAY A. CALDWELL,<sup>1</sup> BARBARA R. GRUBB,<sup>1</sup> ROBERT TARRAN,<sup>1</sup> RICHARD C. BOUCHER,<sup>1</sup>  
MICHAEL R. KNOWLES,<sup>1</sup> and PIERRE M. BARKER<sup>2</sup>

<sup>1</sup>Cystic Fibrosis/Pulmonary Research and Treatment Center, and <sup>2</sup>Department of Pediatrics, The University of North Carolina at Chapel Hill, Chapel Hill, NC 27599

**ABSTRACT** The pathogenesis of cystic fibrosis (CF) airways disease remains controversial. Hypotheses that link mutations in CFTR and defects in ion transport to CF lung disease predict that alterations in airway surface liquid (ASL) isotonic volume, or ion composition, are critically important. ASL  $[\text{Cl}^-]$  is pivotal in discriminating between these hypotheses, but there is no consensus on this value given the difficulty in measuring  $[\text{Cl}^-]$  in the “thin” ASL ( $\sim 30 \mu\text{m}$ ) in vivo. Consequently, a miniaturized solid-state electrode with a shallow depth of immersion was constructed to measure ASL  $[\text{Cl}^-]$  in vivo. In initial experiments, the electrode measured  $[\text{Cl}^-]$  in physiologic salt solutions, small volume (7.6  $\mu\text{l}$ ) test solutions, and in in vitro cell culture models, with  $\geq 93\%$  accuracy. Based on discrepancies in reported values and/or absence of data, ASL  $\text{Cl}^-$  measurements were made in the following airway regions and species. First, ASL  $[\text{Cl}^-]$  was measured in normal human nasal cavity and averaged  $117.3 \pm 11.2 \text{ mM}$  ( $n = 6$ ). Second, ASL  $[\text{Cl}^-]$  measured in large airway (tracheobronchial) regions were as follows: rabbit trachea and bronchus =  $114.3 \pm 1.8 \text{ mM}$ ; ( $n = 6$ ) and  $126.9 \pm 1.7 \text{ mM}$ ; ( $n = 3$ ), respectively; mouse trachea =  $112.8 \pm 4.2 \text{ mM}$  ( $n = 13$ ); and monkey bronchus =  $112.3 \pm 10.9 \text{ mM}$  ( $n = 3$ ). Third,  $\text{Cl}^-$  measurements were made in small (1–2 mm) diameter airways of the rabbit ( $108.3 \pm 7.1 \text{ mM}$ ,  $n = 5$ ) and monkey ( $128.5 \pm 6.8 \text{ mM}$ ,  $n = 3$ ). The measured  $[\text{Cl}^-]$ , in excess of 100 mM throughout all airway regions tested in multiple species, is consistent with the isotonic volume hypothesis to describe ASL physiology.

**KEY WORDS:** cystic fibrosis • defensins • ion-selective electrodes • ionic strength • mucus

## INTRODUCTION

Cystic fibrosis (CF)\* is a lethal genetic disease that results from mutations in the gene that expresses the CFTR protein. Although it is well established that this protein is a cAMP-regulated  $\text{Cl}^-$  channel and regulator of other ion channels (for reviews see Schwiebert et al., 1999; Sheppard and Welsh, 1999), the physiological role of CFTR in airway epithelia is less understood. Consequently, whereas progressive lung disease accounts for  $>90\%$  of the mortality in CF (Davis et al., 1996), the primary cellular mechanisms of CF lung disease remain controversial.

Considerable attention has focused on the role of the CFTR protein in regulating the volume and/or ion composition of the  $\sim 30\text{-}\mu\text{m}$  deep airway surface liquid (ASL) layer, which provides the first line of host-defense against inhaled pathogens (for reviews see Bals et al., 1999; Wine, 1999). Two hypotheses that link mutations in CFTR to defects in ASL volume and/or ion composition have been proposed. The “high salt” (compositional) model predicts the normally low ASL  $[\text{Cl}^-]$  (i.e.,

$[\text{NaCl}] \sim 50 \text{ mM}$ ) is elevated in CF ( $>100 \text{ mM NaCl}$ ) because of defective transepithelial  $\text{Cl}^-$  absorption (Smith et al., 1996; Wine, 1999). Salt-sensitive airway host-defense peptides (defensins) function effectively in bacterial killing below 50 mM  $[\text{NaCl}]$ . In CF, defensins are fully inhibited at  $[\text{NaCl}] > 100 \text{ mM}$  (Goldman et al., 1997), thus, providing a permissive environment for chronic bacterial infection (Bals et al., 1998). In contrast, the “low volume” model predicts that the ASL  $[\text{Cl}^-]$  is isosmotic with respect to plasma (human plasma  $[\text{Cl}^-] \sim 104 \text{ mM}$ ) in both normal and CF airways. However, the ASL volume is reduced in CF because of volume hyperabsorption (Matsui et al., 1998; Wine, 1999) due to the combined effects of  $\text{Na}^+$  hyperabsorption (Boucher et al., 1986; Stutts et al., 1995) and failure to secrete  $\text{Cl}^-$  (Tarran et al., 2001a). As a result, reduced mucus hydration adversely affects mucus clearance, and results in inefficient removal of pathogens.

As recently reviewed (Krouse, 2001), it has been difficult to distinguish between these hypotheses based on ASL compositional data from in vitro experiments. Thus, there is a clear need to measure ASL ion composition in vivo. However, it has been difficult to make comprehensive measurements of ASL ion composition, because of the shallow depth of ASL and measurement-induced artifacts. We fabricated miniaturized electrodes with the following features to make measurements informative in discriminating between the two

The online version of this article contains supplemental material.

Address correspondence to Ray A. Caldwell, Cystic Fibrosis/Pulmonary Research and Treatment Center, CB# 7248, University of North Carolina at Chapel Hill, Chapel Hill, NC 27599-7248. Fax: (919) 966-7035; E-mail: ray\_caldwell@med.unc.edu

\*Abbreviations used in this paper: ASL, airway surface liquid; CF, cystic fibrosis; LR, lactated Ringer's solution.

hypotheses described above: (1) sensitivity to  $[\text{Cl}^-]$ , based on the notion that this parameter will reliably estimate the minimum theoretical ASL ionic strength (Note that defensin-ion killing curves are sensitive to ionic strength; Travis et al., 1999); (2) shallow depth of immersion; and (3) thin and flexible to minimize airway trauma. The electrode and reference assembly were tested by measuring the  $[\text{Cl}^-]$  in small volume (in microliter units) test solutions, physiologic salt solutions, and in *in vitro* cell culture models before proceeding to *in vivo* studies.

We then applied the electrode technique to test whether ASL  $[\text{Cl}^-]$  *in vivo* was  $\leq 50$  or  $\geq 100$  mM in a series of experiments selected on the basis of conflicting and/or absent data in the literature on ASL  $[\text{Cl}^-]$ . Because reports that the *in vivo* ASL  $[\text{Cl}^-]$  of nasal airways is  $\geq 100$  mM in normal humans have been criticized as reflecting sampling artifact (e.g., contamination of filter paper by interstitial fluid; Pilewski and Frizzell, 1999),  $\text{Cl}^-$ -sensitive electrodes were used to measure nasal ASL  $[\text{Cl}^-]$  in normal human subjects. Because studies have reported tracheobronchial ASL  $[\text{Cl}^-]$  values that vary widely, particularly in the mouse, (range: 1.3–140 mM) depending on the measurement technique (Bacconnais et al., 1998; Cowley et al., 2000; Jayaraman et al., 2001a), we measured mouse tracheal ASL  $[\text{Cl}^-]$  and for comparison, tracheal and bronchial ASL  $[\text{Cl}^-]$  in rabbits and bronchial ASL in monkeys. Finally, because no *in vivo* ASL ion measurements have been reported from regions likely to be the site of early CF lung disease (Davis et al., 1996), e.g., small airways (bronchioles), ASL  $[\text{Cl}^-]$  measurements were made at this site in two species.

## MATERIALS AND METHODS

### Humans

Nasal ASL  $[\text{Cl}^-]$  in normal human subjects (23–47 yr; five males and one female) was measured in either nostril, before and after a 10–15-min nasal occlusion with nostril clips. The protocol was approved by the University of North Carolina (UNC) Human Rights Committee.

### Animals

New Zealand White rabbits (either sex, 5–6 kg; Robinson Services) were anesthetized with 5% (vol/vol) isoflurane (Burns Veterinary Supply) and 95% oxygen using an isoflurane vaporizer (Anesco). The gas mixture was humidified by bubbling it through 300 ml of distilled, deionized  $\text{H}_2\text{O}$  contained in a 500-ml filtration flask. The anesthetic was delivered to the rabbit with a mask covering the mouth and nose connected to the flask via a flexible plastic tube (5 mm i.d.  $\times$  1 m). Adult male rhesus monkeys (*Macaca mulatta*, 11–22 kg) were sedated with ketamine (15 mg/kg) for endotracheal intubation and maintained under anesthesia with 1.5–2.5% (vol/vol) isoflurane in oxygen during experiments. Due to concerns that endotracheal intubation could affect the tracheal ASL  $[\text{Cl}^-]$ , tracheal electrode recordings were not attempted in monkeys. Mice (C57-BL6; 12–24 wk) were anes-

thetized with xylazine (30 mg/kg) and ketamine (75 mg/kg) administered subcutaneously. Mice were placed supine on a heating pad ( $\sim 38^\circ\text{C}$ ) and a midline incision was made under the chin that extended to the sternum ( $\sim 1.5$  cm). Next, the trachea was exposed with blunt dissection of the surrounding connective tissue. A tracheostomy was performed, and the lower trachea (caudal) was cannulated with PE-50 tubing (0.58 mm i.d.  $\times$  0.98 mm o.d.; Becton Dickinson) and secured in place with suture. Protocols were approved by the UNC Institutional Animal Care and Use Committee.

### $\text{Cl}^-$ -electrode Sensor and Reference Assembly

The  $\text{Cl}^-$ -electrode sensor is illustrated in Fig. 1 A. Both reference and sensor electrodes were prepared from Teflon-insulated Ag wire (bare wire diam, 127  $\mu\text{m}$   $\times$  99 cm; California Fine Wire). Approximately 2 mm of Teflon was removed from the wire ends for depositing the  $\text{Cl}^-$ -sensing AgCl layer. The AgCl layer was deposited by immersing the wires in 5% (wt/vol)  $\text{NaHClO}_3$  solution for  $\sim 20$  min. Wires were rinsed with distilled, deionized water and allowed to dry for at least 5 h before use.

The sensor and reference electrodes were inserted into PE-50 tubing (94 cm long), which served as the catheter. A reference port was made  $\sim 5$  mm from the sensor end of the catheter using a 30-gauge needle. The reference electrode was recessed 1–3 cm from the sensing end of the catheter. The sensor electrode extended 0.5–1 cm outside the catheter.

The catheter containing the electrodes was inserted into the suction channel (1.0-mm diam) of a pediatric bronchoscope (3-mm diam o.d.; Type 3C10; Olympus) in a retrograde manner to avoid damaging the  $\text{Cl}^-$ -sensor electrode. The catheter and wires that emerged from the top of the bronchoscope near the eyepiece were fitted into a three-way stopcock valve (Medex). Electrodes were connected to an electrometer (model FD 223; World Precision Instruments) via a screw-type terminal connector secured to the bronchoscope.

Because a constant  $[\text{Cl}^-]$  is required to maintain a stable Ag/AgCl reference electrode voltage and because of concerns that the commonly used flowing KCl reference solution could contaminate the  $\text{Cl}^-$  measurements, a KCl- $\text{KNO}_3$  double liquid junction reference assembly was constructed (Bailey, 1980). This assembly was achieved by encapsulating the AgCl tip of the reference electrode in a small plastic sheath ( $\sim 180$   $\mu\text{m}$  i.d.  $\times$  1 cm) containing 5% agar (wt/vol) dissolved in 3 M KCl, saturated with AgCl. The sheath was sealed to the Teflon insulation surrounding the reference electrode with a small drop of quick drying adhesive (Elmer's). Next, the PE-50 catheter was backfilled with 1 M  $\text{KNO}_3$  by applying suction using a syringe connected to the stopcock.

The  $\text{KNO}_3$  reference solution flow-rate was minimized by filling the sensing end of the catheter with  $\sim 1$  cm of 5% agar dissolved in 1 M  $\text{KNO}_3$ . Dental wax (Heraeus Kulzer Inc.) was applied to the catheter tip to mechanically stabilize the column of agar and the sensing electrode, and to restrict the reference solution flow to reference port. The reference solution flow-rate (starting from a 91-cm column height) was 16 nl/min ( $r^2 = 0.986$ ,  $n = 4$ –7 measurements) and could be shut off (e.g., during *in vivo* measurements) by closing a valve attached to the open port of the stopcock. The flowing reference solution was used to minimize the transient liquid junction potential arising from the modest solution volume carried over in the reference port during solution-switches with the calibration procedure.

### $\text{Cl}^-$ -electrode Calibration and Test Solutions

Electrode voltages were recorded in 30-, 100-, and 150-mM  $\text{Cl}^-$  standard solutions. In some experiments, a 10-mM  $\text{Cl}^-$  standard also was used. All calibrations were performed at  $37^\circ\text{C}$  in a stan-

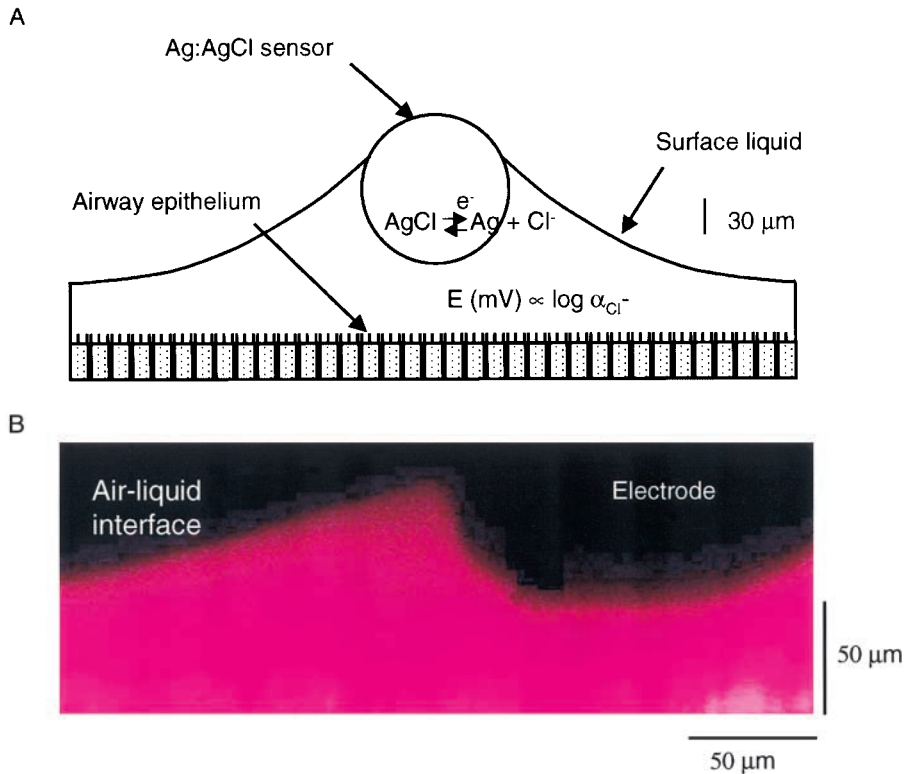


FIGURE 1.  $\text{Cl}^-$ -electrode sensor used for ASL  $\text{Cl}^-$  measurements. (A) Cross-sectional view of the Ag/AgCl sensor and the air–surface liquid profile above airway epithelium is illustrated. ASL  $[\text{Cl}^-]$  is obtained from the electrode voltage (Eq. 1) developed from the electrochemistry at the electrode–electrolyte interface. The low impedance of the interface does not require the electrode to be totally immersed for  $\text{Cl}^-$  measurement. The illustrated air–liquid radius of curvature is from confocal imaging (see below). The illustrated surface liquid height at the edge of the epithelium is from mouse trachea (Jayaraman et al., 2001a). For clarity, the PE-50 catheter containing the reference electrode is not shown. (B) Confocal image of the surface liquid–electrode interface. The electrode-induced radius of curvature was 373  $\mu\text{m}$ .

dard heating block (VWR Scientific) unless otherwise noted. The sample  $[\text{Cl}^-]$  was derived from the sample electrode voltage and the slope and y-intercept parameters obtained from the least-squares fit of the Nernst equation to the electrode voltages recorded in the  $\text{Cl}^-$  standard solutions:

$$E = 2.3(RT/F)\log(\gamma_{\text{Cl}}[\text{Cl}^-]) + C, \quad (1)$$

where  $E$  is the electrode voltage (in millivolt units),  $R$  is the gas constant,  $T$  is absolute temperature,  $F$  is Faraday's constant,  $\gamma_{\text{Cl}}$  is the  $\text{Cl}^-$  activity coefficient, and  $C$  is the y-intercept. The ionic strength of the  $\text{Cl}^-$  standard solutions was adjusted to 150 mM with sodium acetate to fix  $\gamma_{\text{Cl}}$  so that the  $\text{Cl}^-$ -electrode response was proportional to  $\log[\text{Cl}^-]$ . By convention,  $[\text{Cl}^-]$  rather than activity is reported for comparative purposes.

Electrode drift (in millivolt/minute) is reported as the slope of the linear least-squares regression of the electrode response in 100 mM  $\text{Cl}^-$  before and after sampling the test solution. Data obtained from electrodes that drifted  $>0.5$  mV/min or exhibited poor responses to the  $\text{Cl}^-$  standards (slopes  $< 52$  mV at  $37^\circ\text{C}$ ) were excluded. The accuracy of the  $\text{Cl}^-$ -electrode measurements was assessed with several physiologic salt solutions and in small volumes of test solution.

#### *In Vitro Measurements in Small Volumes*

$\text{Cl}^-$  measurements were performed in 7.6  $\mu\text{l}$  of a 100-mM  $\text{Cl}^-$  standard solution spread within the border of a circle (diam, 17.8 mm) inscribed on a metal support to simulate a representative ASL depth ( $\leq 30$   $\mu\text{m}$ , modeled as a cylinder) reported in vitro (Matsui et al., 1998). Evaporative  $\text{H}_2\text{O}$  loss from the small sample volume was estimated by applying 7.6  $\mu\text{l}$  of the solution to filter paper (18-mm diam; Whatmann) and measuring the weight change over time. It is assumed that the rate of evaporative  $\text{H}_2\text{O}$  loss from the filter paper and metal surface is not different under identical conditions (e.g.,  $23^\circ\text{C}$ , 1 atm, 45% relative humidity).

#### *In Vitro Cl<sup>-</sup> Measurements in Cultured Canine Bronchial Epithelium under Fully Humidified Conditions*

Canine bronchial epithelial cells were cultured on 12-mm Transwell-Col supports (Costar Corp.), grown under air–liquid interface conditions, and studied when confluent (12–14 d postseeding; Matsui et al., 1998).  $\text{Cl}^-$  measurements with Ag/AgCl electrodes were made under conditions similar to those described by Matsui et al. (1998). Briefly, the apical cell surface was washed three times with 100  $\mu\text{l}$  of PBS solution. Next, 100  $\mu\text{l}$  of PBS solution was applied at  $t = 0$  min (predicted surface liquid height  $< 100$   $\mu\text{m}$ ; extrapolated from measurements by Tarran and Boucher, 2001) and the cultures were placed in a humidity chamber consisting of a styrofoam-insulated box ( $23 \times 18 \times 12$  cm) containing a transparent Plexiglas cover. Chamber temperature and relative humidity were measured using a combination temperature-humidity probe (model HI9065C; Hanna Instruments). Cultures were maintained at  $\sim 37^\circ\text{C}$  with a thermostatically controlled heating block (Fisher Scientific). Humidity was maintained (relative humidity  $\sim 100\%$ ) with  $\text{H}_2\text{O}$ -saturated sponges placed inside the chamber. The  $\text{Cl}^-$ -electrode and reference assembly were modified to facilitate measurement of  $\text{Cl}^-$  in cell culture. Shortened electrodes ( $\sim 45$  cm) were prepared with the PE-50 catheter bent at  $90^\circ$ ,  $\sim 5$  cm from the sensing end, so that the sensor, reference port, and the plane of the surface liquid were in parallel to facilitate contact between the electrode and surface liquid. Once cell cultures had reached the desired temperature and humidity and electrode calibration were complete ( $t = 150$ – $210$  min), the catheter was visually guided onto the epithelial surface through a small slit in the Plexiglas cover. A micromanipulator was used for fine adjustments to the electrode position along the z-axis until a stable electrode voltage was recorded, indicating the sensor was contacting the surface liquid. For continuous observation of electrode placement, condensation on the Plexiglas was prevented by warming the cover with

minimal current passed through Pt-Ir wire secured to the Plexiglas using a variable DC power supply.

### *In Vitro Studies Imaging the ASL-electrode Interface*

The surface liquid (air-liquid interface) profile was imaged using xz-scanning confocal microscopy as previously described (Matsui et al., 1998). Briefly, 100  $\mu$ l of PBS containing 2 mg/ml Texas red was applied to the apical surface of cultured bronchial epithelia. Next, a 1-cm length of the Cl<sup>-</sup>-sensing electrode was placed in the surface liquid, and images were acquired confocally and analyzed with Metamorph (Universal Image Co.) to estimate the electrode-induced radius of curvature formed at the surface liquid-electrode interface (Fig. 1 B).

### *Studies of Human, Rabbit, and Monkey ASL [Cl<sup>-</sup>] In Vivo*

The bronchoscope was visually guided into airways for in vivo measurements in humans, rabbits, and monkeys. Next, the catheter was advanced from the bronchoscope, observed to touch the wall of the airway, and the electrode voltage was recorded. In some experiments, a PE-10 (0.28 i.d.  $\times$  73-cm) catheter was secured to the outside of the bronchoscope for superfusing Cl<sup>-</sup> standard solutions into the airway.

The possibility of a Donnan potential arising from charged mucins in the space between the tip of the sensing electrode and reference port was evaluated in vivo using two Ag/AgCl electrodes extended 0.5–2 cm from the end of the catheter. The distance between the electrodes was similar to the length between the reference port and the sensing electrode for Cl<sup>-</sup> measurements.

### *Studies of Mouse Tracheal ASL [Cl<sup>-</sup>]*

For mouse studies, Cl<sup>-</sup>-electrode and transepithelial potential measurements were made with the catheter placed 5–8 mm in the trachea (cephalic) distal to the larynx. Transepithelial potential was measured between the catheter reference port and a subcutaneous electrode identical to the Cl<sup>-</sup> reference electrode assembly described above. Tracheal lumen temperature ( $31.9 \pm 0.5^\circ\text{C}$ ,  $n = 9$ ) was measured immediately after electrode recordings with a copper-constantan (type T) thermocouple thermometer (Cole Parmer).

### *Chemicals*

K<sup>+</sup> and Na<sup>+</sup> chloride salts, and sodium acetate were purchased from Mallinckrodt. KNO<sub>3</sub>, and AgCl were obtained from Sigma-Aldrich. All salts were at least ACS grade. Texas red was purchased from Molecular Probes. The physiologic salt solutions, Ham's F12 ([Cl<sup>-</sup>] = 136 mM; Cat No. 21700) and FBS, were purchased from GIBCO BRL. Lactated Ringer's ([Cl<sup>-</sup>] = 109 mM) was purchased from Baxter. PBS was prepared from stock solutions and contained the following (in mM): 137 NaCl, 2.7 KCl, 7.5 Na<sub>2</sub>HPO<sub>4</sub>  $\cdot$  7 H<sub>2</sub>O, and 1.5 KH<sub>2</sub>PO<sub>4</sub>, pH  $\sim$ 7.3. In selected experiments, Cl<sup>-</sup>-electrode measurements were performed in 10 mM HEPES-buffered Ringer's solution, pH 6–8 adjusted with NaOH, and in Ringer's solution containing 28 mM NaHCO<sub>3</sub>, pH 8.12.

### *Data Acquisition and Analysis*

All electrometer output voltages were digitized at 256-kHz (industry set burst-rate). For most experiments, the time-averaged signal was acquired at 10-Hz (throughput rate) with a 16-bit analogue-digital converter (Dataq) and a Pentium computer running commercially available data acquisition software (Dataq). Electrode kinetics were measured from responses acquired at 0.24 kHz throughput rate. Sigma Plot (v4.0; SPSS) was used for data presentation and analysis. Data are reported as mean  $\pm$

SEM, with  $n$  representing the number of animals or in vitro measurements as appropriate. Human nasal liquid Cl<sup>-</sup> concentrations before and after nasal occlusion were compared using a paired  $t$  test (SigmaStat, v2.0, SPSS). A P value of less than 0.05 was considered statistically significant.

### *Online Supplemental Material*

In some experiments, placement of the Cl<sup>-</sup>-electrode in monkey and rabbit airways was videotaped (VHS; Mitsubishi Digital Electronics) using a camera (model OTU-SC; Olympus) attached to the bronchoscope. Representative electrode placements in rabbit trachea, main bronchus, and in a small airway are shown. Video is available at <http://www.jgp.org/cgi/content/full/119/1/1/DC1>.

## RESULTS

### *Electrode Responsiveness and Accuracy in Standardized Solutions*

Several salt solutions were studied to characterize the electrode behavior in solutions comprised of various ionic compositions and to assess the accuracy of the Cl<sup>-</sup> concentrations predicted from the electrode responses. A representative recording is shown in Fig. 2 A. Before immersion in the test solution, the electrode response was calibrated in 30-, 100-, and 150-mM Cl<sup>-</sup> standard solutions after the voltage was nulled in a 10-mM Cl<sup>-</sup>-containing solution.

After the standardization procedure and after returning the catheter to the 100-mM Cl<sup>-</sup> standard solution, the steady-state voltage (Fig. 2 A, 8–10 min) was within 1 mV of the initial steady-state value recorded in this solution. Subsequently, the electrode response in the lactated Ringer's (LR) test solution was recorded. The voltage response in this solution was similar to the value recorded in the 100-mM Cl<sup>-</sup> standard. To assess the stability of the electrode response after sampling the test solution, voltages were recorded in 100- and 30-mM Cl<sup>-</sup> standards, respectively.

Fig. 2 B shows the analysis of the voltage responses obtained in the Cl<sup>-</sup> standards and in the LR solution in A. The open circles and squares represent the electrode voltages, averaged over the last 10–30 s in each of the calibration standards, before and after sampling the LR solution, respectively. The Nernst equation (Fig. 2 B, solid line, Eq. 1) was fitted to the open circles. The average LR [Cl<sup>-</sup>], determined from the sample responses like shown in Fig. 2, was  $111.8 \pm 0.8$  mM ( $n = 4$ ). This value is 2.6% larger than the LR [Cl<sup>-</sup>] listed by the supplier.

The electrode kinetics, sensitivity to changes in [Cl<sup>-</sup>], and drift were evaluated from recordings similar to that shown in Fig. 2 A. The 10–90% rise time ( $t_{10-90}$ ) for the electrode voltage to reach steady state after switching from 100 to 150 mM Cl<sup>-</sup> containing solution was  $0.26 \pm 0.04$  s, but was comparatively slower ( $2.0 \pm 0.2$  s) when the solution switching order was reversed ( $25^\circ\text{C}$ ,  $n = 3$ ). The electrode slope parameter was

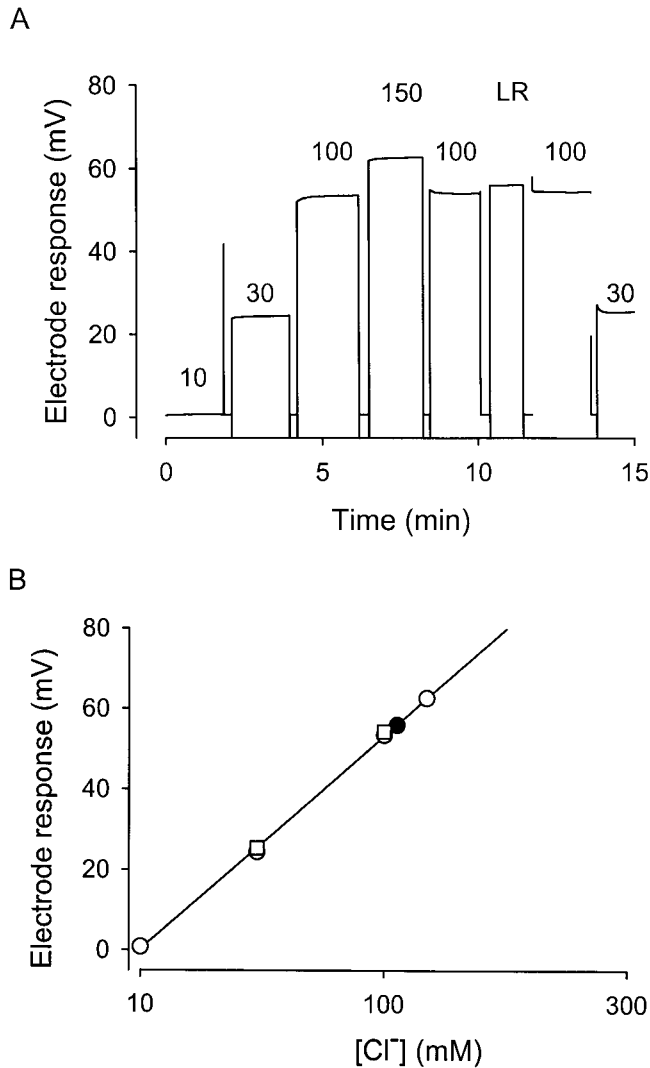


FIGURE 2. Representative electrode recording and analysis used to determine  $[\text{Cl}^-]$  in various salt solutions. (A)  $\text{Cl}^-$ -electrode recording in lactated Ringer's (LR) solution is shown. The electrode response was recorded in  $\text{Cl}^-$  calibration solutions (in millimolar units, labeled above the trace). The electrometer output voltage was zeroed in 10 mM  $\text{Cl}^-$  solution and switched to ground between measurements. (B) The LR  $[\text{Cl}^-]$  (113.0 mM, ●) was determined from the sample voltage response and  $E(\text{mV}) = 52.8 \cdot \log[\text{Cl}^-] - 53.0$  (Eq. 1; solid line fitted to ○ calibration symbols). Open squares partially mask open circles and represent the responses obtained in the calibration standards after LR  $\text{Cl}^-$  measurement. Note log-scale for abscissa. Electrode drift was 0.1 mV/min ( $r^2 = 0.988$ ). For each salt solution, at least three measurements were made in  $\sim 5$ -ml solution volumes (23–25°C).

$56.6 \pm 0.3$  mV ( $r^2 = 0.99$ ;  $n = 33$ ; 37°C), or 0.92 of the theoretical Nernstian slope (Eq. 1). The electrode drift was  $0.15 \pm 0.02$  mV/min ( $r^2 = 0.92$ ,  $n = 29$ , 37°C). Electrode voltages were adjusted for drift as appropriate.

The measured  $\text{Cl}^-$  concentrations in LR, PBS, and Ham's F12 salt solutions were within 1–7% of the listed  $\text{Cl}^-$  values (MATERIALS AND METHODS). Ag/AgCl electrodes exhibit Nernstian responses to changes in  $\text{Cl}^-$

activity from pH 2.0 to 11 (Bailey, 1980). Nevertheless, experiments were performed to specifically assess if pH or  $\text{HCO}_3^-$  affected the accuracy of the  $\text{Cl}^-$ -electrode measurements. The  $[\text{Cl}^-]$  was measured in three HEPES-buffered Ringer's solutions (pH range: 6–8). In addition, the  $[\text{Cl}^-]$  in Ringer's solution containing 28 mM  $\text{NaHCO}_3$  also was measured. The average  $\text{Cl}^-$  values measured in each of these solutions were within 1.7% of the theoretical Ringer's  $[\text{Cl}^-]$  ( $n = 3$  measurements for each solution).

The electrode exhibited stable and reversible voltages in the  $\text{Cl}^-$  calibration solutions after measurement in the test solution. Stable recordings also were obtained in Ham's F12 supplemented with 10% FBS. The sensitivity and reproducible voltages of the electrode to changes in  $\text{Cl}^-$  after measurement in the test solution indicates the electrode was not fouled by interfering ions. Thus, the  $\text{Cl}^-$ -electrode performed with reasonable accuracy in physiologic salt solutions designed to mimic the ASL ionic milieu.

#### *Cl<sup>-</sup> Measurements in an In Vitro Model ASL Test System with Standardized Solutions*

Although recent measurements of ASL depth in vivo exceed 50  $\mu\text{m}$ , depths reported from cell culture models are  $< 25$   $\mu\text{m}$  (Verkman, 2001). We chose to evaluate the electrode performance in a test solution  $\leq 30$   $\mu\text{m}$  deep, reflecting the more shallow in vitro ASL depth. The measured  $[\text{Cl}^-]$  was systematically higher than the  $\text{Cl}^-$  value in the original volume of test solution by  $5.2 \pm 0.5\%$  ( $n = 3$ ), which likely resulted from evaporative  $\text{H}_2\text{O}$  loss from the small sample volume. To assess the evaporation rate, the change in filter paper (18-mm diam) weight containing the same volume of test solution ( $t = 0$  min) was recorded for up to 3 min. The rate of the  $[\text{Cl}^-]$  increase expected from evaporative  $\text{H}_2\text{O}$  loss was  $10.6\% \text{ min}^{-1}$  ( $r^2 = 0.966$ ,  $n = 3$ , 25°C). Given the 0.5–1-min delay between removing the catheter from the calibration standard and sampling the test solution, the  $\text{Cl}^-$  measurements fall within the range of concentrations predicted when considering evaporative water loss from the small sample volume.

#### *Cl<sup>-</sup> Measurements of ASL in a Tissue Culture Model System*

To assess the accuracy of the  $\text{Cl}^-$ -electrode measurements in cell culture and in the absence of evaporative  $\text{H}_2\text{O}$  loss, measurements were made in PBS covering cultured canine bronchial epithelium. Cultures were placed in a specially designed humidity chamber (relative humidity range: 96–100%; temperature  $\sim 37^\circ\text{C}$ ) that allowed electrode access via a small opening in the top. Measurements were made 2–3.5 h after washing the apical surface with PBS to provide sufficient time for temperature and humidity to attain equilibrium. Individual  $\text{Cl}^-$  values varied above and below the theoret-

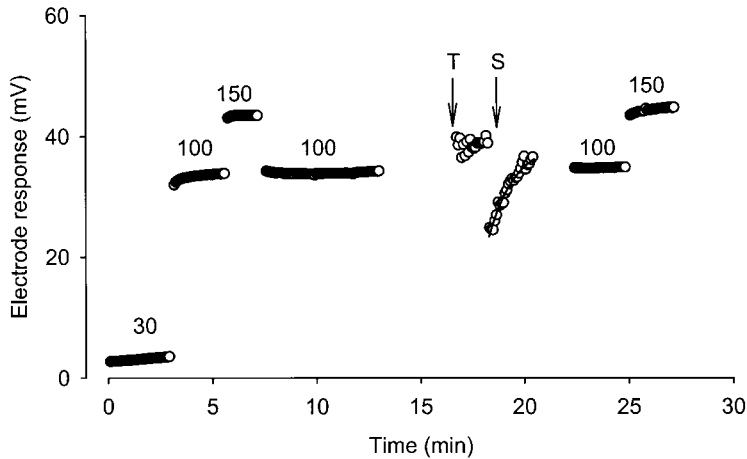


FIGURE 3. ASL  $[\text{Cl}^-]$  is decreased after 30 mM  $\text{Cl}^-$  instillation. Tracheal  $\text{Cl}^-$ -electrode recording is indicated (T) after the calibration procedure (see Fig. 2 legend). The ASL  $[\text{Cl}^-]$  decreased from 121.6 to 65.0 mM after instilling 55  $\mu\text{l}$  ( $37^\circ\text{C}$ ) of the low  $\text{Cl}^-$  solution (S). The ASL  $\text{Cl}^-$  concentrations were obtained from  $E(\text{mV}) = 57.4 \cdot \log[\text{Cl}^-] - 81.2$ . Subsequently, the electrode voltage recovered. The recovery was well described by  $E(\text{mV}) = 23.3 + 15.7(1 - e^{-t/47.5\text{s}})$  (solid curve, adjusted  $r^2 = 0.968$ ). Unfilled circles represent data points collected at 5-s intervals to illustrate clearly the fitted kinetic model.

ical PBS  $[\text{Cl}^-]$ , ranging from 136.7 to 150.8 mM. The average  $[\text{Cl}^-]$  was  $141.6 \pm 4.6$  mM ( $n = 3$ ), or 101% of the theoretical PBS  $[\text{Cl}^-]$ .

#### Physical Interaction of the Solid-state $\text{Cl}^-$ -electrode and ASL

Because the electrode must contact the ASL for  $\text{Cl}^-$  measurement, the electrode and ASL profile were imaged with confocal microscopy. From the radius of curvature (Fig. 1 B) and the in vitro ASL surface tension (Tarran et al., 2001a), the electrode pressure calculated from LaPlaces' law was  $182.3 \text{ N/m}^2$ . This value is 0.21–0.72 of the values reported for filter paper and polyethylene catheters used for ASL collection, respectively (Landry et al., 2000). From the apparent hydraulic conductivity value reported for bovine tracheal epithelium (Durand et al., 1981), and assuming all fluid flow is radially directed across the airways epithelium, the pressure exerted by the electrode would result in a volume flux =  $7.85 \text{ pl cm}^{-2} \text{ s}^{-1}$ . This would contribute 11.7 pl of volume to the apical surface in 100 s, which is  $<0.02\%$  of the total volume occupied by a slab of ASL  $2000 \times 743 \times 50 \mu\text{m}$  (electrode sensor length  $\times$  surface liquid curve diameter  $\times$  ASL height). Thus, the electrode results in minimal perturbation to ASL volume.

#### Characterization of Electrode Performance In Vivo in the Rabbit Trachea

To assess the accuracy of the electrode measurement in vivo, the electrode response was recorded continuously before (basal values), during, and after superfusion of a “low”  $\text{Cl}^-$  standard solution onto the luminal surface of rabbit trachea (Fig. 3). After calibration, the electrode was briefly rinsed with deionized  $\text{H}_2\text{O}$  ( $37^\circ\text{C}$ ), and the bronchoscope containing the catheter electrode was advanced into the lumen of the airway. Next, the catheter was extended from the bronchoscope by  $\sim 2$  cm and gently placed along the tracheal wall. The letter “T” (Fig. 3) denotes the initiation of the tracheal recording. During the first 21 s of the recording, the voltage response

oscillated by 3–5 mV (range: 36–41 mV) with a frequency of 14–18  $\text{min}^{-1}$  that paralleled the tracheal oscillatory motion observed through the bronchoscope. The electrode response, measured from 18.0 to 18.3 min, was  $38.4 \pm 0.4$  mV (mean  $\pm$  SD, range: 38.0–38.5 mV), corresponding to a tracheal ASL  $[\text{Cl}^-] = 121.6$  mM.

Next, 55  $\mu\text{l}$  of the 30 mM  $\text{Cl}^-$  calibration solution ( $37^\circ\text{C}$ ) was superfused onto the tracheal wall (Fig. 3, S) and a precipitous decrease in the electrode voltage occurred, which is consistent with a reduction in the ASL  $[\text{Cl}^-]$ . The nadir of the voltage response (23 mV) occurred 6 s after beginning the superfusion, corresponding to a  $[\text{Cl}^-] = 65$  mM. Subsequently, the electrode voltage returned toward the baseline value. The recovery was well described by a single exponential model (time constant = 47.5 s; Fig. 3, solid curve). The steady-state voltage obtained from the model was 39.0 mV, which is in good agreement with the electrode output measured just before superfusion. Thus, the solid-state sensor provides rapid and direct measurement of changes in ASL  $[\text{Cl}^-]$  in real time. Subsequently, the bronchoscope was removed from the airway and the electrode response was recorded in 100- and 150-mM  $\text{Cl}^-$  standard solutions to assess the stability of the electrode response in these solutions. The steady-state voltage responses in the  $\text{Cl}^-$  calibration solutions following the in vivo recording were indistinguishable from those obtained before sampling the ASL  $[\text{Cl}^-]$ , indicating that the electrode was not fouled by the in vivo measurement.

The nadir of the tracheal electrode response after instilling the 30-mM  $\text{Cl}^-$  solution was 23 mV larger than the voltage recorded in the 30-mM  $\text{Cl}^-$  calibration solution. To examine if this difference resulted from a Donnan potential arising from fixed charges (i.e., mucins) on the airway surface, the voltage between two Ag/AgCl electrodes (spaced  $\sim 0.5$  cm apart) in trachea and small (1–2-mm diam) airways was recorded. The tracheal and small airway responses varied in polarity and were  $0.11 \pm 0.41$  and  $1.0 \pm 1.2$  mV ( $n = 3$ ), respectively. Although

these measurements do not account for the liquid junction potential between the reference and sample solution, it is unlikely that a junction potential, Donnan potential, or the combination of these offset voltages can account for the difference in the electrode response observed between the calibration solution and the in vivo recording after superfusion (see DISCUSSION). Rather, the electrode response likely reflects the aggregate  $[\text{Cl}^-]$  after mixing of the low  $\text{Cl}^-$  standard solution with the more concentrated ASL  $[\text{Cl}^-]$ . This notion is supported by a similar experiment in vivo where the electrode voltage was recorded after tracheal instillation of a 150-mM  $\text{Cl}^-$ -containing solution. The electrode voltage was within 2.2 mV (i.e.,  $\sim 10\%$  underestimation of the calibration  $[\text{Cl}^-]$ ) of the response recorded in the calibration solution (not shown).

#### *In Vivo $\text{Cl}^-$ Measurements in Human Nasal ASL*

The nose is a commonly used site to study human ASL ion composition (Hull et al., 1998; Knowles et al., 1997) and airway epithelial ion transport in vivo. Previously, nasal liquid  $\text{Cl}^-$  measurements have been based on fluid collected with absorptive material (i.e., filter paper) with and without nasal occlusion. Thus, to compare  $\text{Cl}^-$ -electrode measurements of the nasal liquid  $[\text{Cl}^-]$  with previously reported values, the nasal liquid  $\text{Cl}^-$  was measured with the catheter placed under the inferior turbinate before and after at least 10 min of nasal occlusion from the same subject. The postocclusion nasal liquid  $[\text{Cl}^-]$  was  $117.3 \pm 11.2$  mM ( $n = 6$ ) and was similar to that previously reported with filter paper studies (Knowles et al., 1997; see DISCUSSION). As expected, the electrode detected a comparatively higher nasal  $[\text{Cl}^-]$  ( $148.8 \pm 13.4$  mM;  $P < 0.05$ ) during continuous nasal breathing, i.e., preocclusion, of room air ( $25^\circ\text{C}$ , 42% relative humidity).

#### *ASL $\text{Cl}^-$ Measurements in Rabbit Trachea and Bronchi and Monkey Bronchi*

The rabbit tracheal ASL  $[\text{Cl}^-]$  was measured as described (and see Fig. 3), and averaged  $114.3 \pm 1.8$  mM ( $n = 6$ ). Fig. 4 shows a representative in vivo  $\text{Cl}^-$ -electrode recording in rabbit right main bronchus. After the standardization procedure, the electrode was placed along the bronchial wall and the response was recorded for 66 s. The rabbit bronchial ASL  $[\text{Cl}^-]$ , derived from the time-averaged bronchial voltage and the Nernstian fit parameters, was 124.0 mM. The steady-state voltage responses in the  $\text{Cl}^-$  calibration solutions after the in vivo recording were indistinguishable from those obtained before sampling the ASL. The ASL  $[\text{Cl}^-]$  in rabbit first to third generation bronchi was  $126.9 \pm 1.7$  mM ( $n = 3$ ). In monkey, second to third generation bronchi, ASL  $[\text{Cl}^-]$  was  $112.3 \pm 10.9$  mM ( $n = 3$ ).

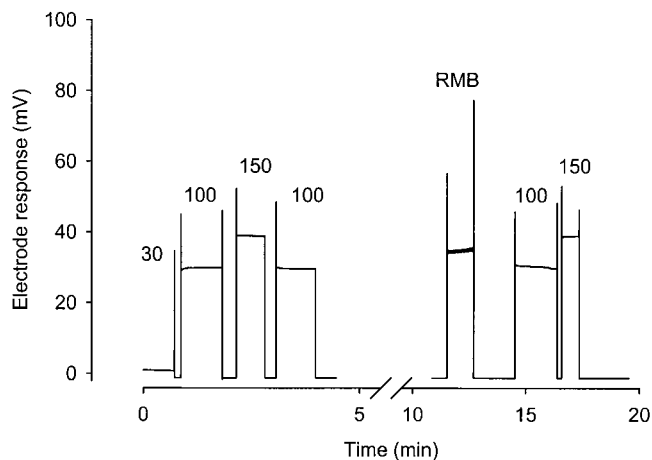


FIGURE 4. Right main bronchus (RMB)  $\text{Cl}^-$ -electrode recording in rabbit. After electrode calibration (0–5 min), the voltage response during the 66-s RMB recording was  $34.7 \pm 0.3$  mV (mean  $\pm$  SD; range: 34.1–35.7 mV) corresponding to a  $[\text{Cl}^-] = 124.0$  mM ( $E(\text{mV}) = 54.8 \cdot \log[\text{Cl}^-] - 80.1$ ;  $r^2 = 0.999$ ). Stable responses were obtained in  $\text{Cl}^-$  standard solutions (15–17 min) after the RMB measurement.

#### *Transepithelial Potential and ASL $\text{Cl}^-$ Measurements in Mouse Trachea*

Previous reports of mouse tracheal  $[\text{Cl}^-]$  values vary widely, raising the possibility that these measurements were contaminated by water vapor condensate (Cowley et al., 2000) and/or  $\text{Cl}^-$  from interstitial and/or plasma compartments resulting from airway epithelial damage (Pilewski and Frizzell, 1999). Therefore, the integrity of the epithelial barrier was functionally assessed in mice by measuring the transepithelial electrical potential together with the  $\text{Cl}^-$ -electrode recordings. A representative experiment is shown in Fig. 5. Both the transepithelial electrical potential (Fig. 5 A, arrow) and  $\text{Cl}^-$ -electrode voltage were stable during the 4-min recording (Fig. 5 B). The mouse transepithelial electrical potential was  $8.4 \pm 0.8$  mV (lumen negative,  $n = 13$ ), which is similar to the values previously reported (Takahashi et al., 1993). Mouse tracheal  $[\text{Cl}^-]$  was  $112.8 \pm 4.2$  mM ( $n = 13$ ). Taken together, it is unlikely that the  $\text{Cl}^-$ -electrode measurements were contaminated by liquids from other compartments resulting from electrode-induced epithelial damage.

#### *Rabbit and Monkey Small Airways*

Because CF lung disease begins in the small airways, and because two contrasting models of ASL physiology predict substantial differences in the ASL  $[\text{Cl}^-]$ , knowledge of the ASL  $[\text{Cl}^-]$  in small airways is fundamental to understanding the ion composition in this region. The ASL  $[\text{Cl}^-]$  measured in the small airways (1–2-mm diam) of rabbit was  $108.3 \pm 7.1$  mM ( $n = 5$ ), and in

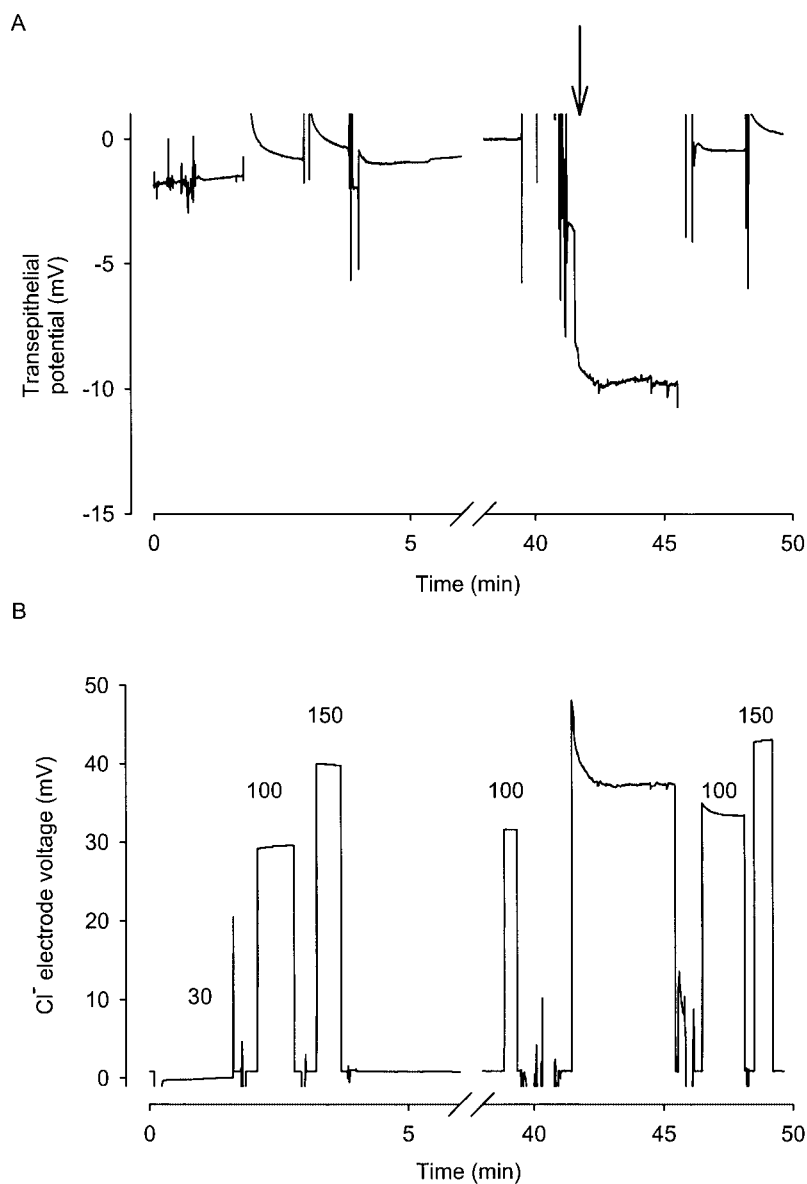


FIGURE 5. Transepithelial potential measurement during  $\text{Cl}^-$ -electrode recording in mouse trachea. (A) Tracheal epithelial integrity was assessed during  $\text{Cl}^-$ -electrode recordings by measuring the transepithelial potential ( $\downarrow$ ). Transepithelial potential was stable and remained polarized (lumen negative) throughout the experiment. (B) Tracheal  $\text{Cl}^-$ -electrode voltage recorded simultaneously with the transepithelial potential in A. The tracheal  $[\text{Cl}^-]$  (from  $E(\text{mV}) = 56.6 \cdot \log[\text{Cl}^-] - 83.6$ ;  $r^2 = 0.999$ ) was 120 mM. Electrode drift was 0.08 mV/min ( $r^2 = 0.94$ ). Lumenal tracheal temperature was  $31.9 \pm 0.5^\circ\text{C}$ , ( $n = 9$ ). Calibration solution temperatures were adjusted appropriately. Break in abscissa corresponds to 32 min during the mouse anesthesia and surgical procedure. Portions of the figure were suppressed between switching the calibration solutions.

monkey was  $128.5 \pm 6.8$  mM ( $n = 3$ ). These values are similar to the ASL  $[\text{Cl}^-]$  measured in the larger airways.

ASL  $\text{Cl}^-$  values for mouse, rabbit, and monkey are shown in Fig. 6. For comparison, the human nasal liquid  $[\text{Cl}^-]$  also is shown. The ASL  $[\text{Cl}^-]$  values in large and small animals and humans (after nasal occlusion) were similar and averaged  $>100$  mM (range: 108–129 mM).

## DISCUSSION

### *Solid-state $\text{Cl}^-$ -electrode Approach to Measure ASL $[\text{Cl}^-]$ In Vivo*

ASL ion composition analysis has largely relied on liquid sampled with absorptive materials (Joris et al., 1993; Knowles et al., 1997; Hull et al., 1998). This procedure has been criticized for wicking fluid and elec-

trolytes from other compartments (e.g., interstitium; Erjefalt and Persson, 1990; Pilewski and Frizzell, 1999). Moreover, the analysis requires lengthy and meticulous laboratory procedures for sample extraction (Joris et al., 1993; Knowles et al., 1997). On the other hand, the technology to perform rapid and direct measurement of  $\text{Cl}^-$  with solid state, Ag/AgCl electrodes in a wide range of solutions of biological interest has existed for over three decades (Hansen et al., 1968; Kopito and Shwachman, 1969; Koryta, 1975). However, measuring the ASL ionic composition in vivo with commercially available ion-selective electrodes (i.e.,  $>1$ -mm diam) has been formidable because of the shallow depth of ASL and limited access to distal airways where CF lung disease originates (Davis et al., 1996). The solid-state  $\text{Cl}^-$ -electrode we developed (Fig. 1) preserved the sensitivity and specificity for  $\text{Cl}^-$ , but was sufficiently small



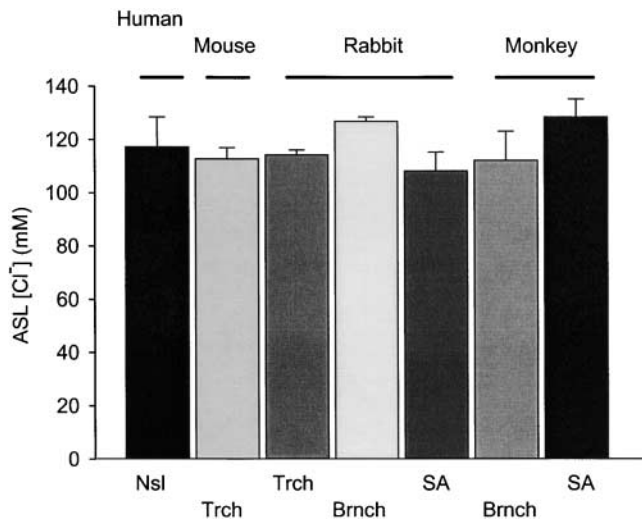


FIGURE 6. Summary ASL  $\text{Cl}^-$  values in various species. Mouse trachea (Trch,  $112.8 \pm 4.2$  mM,  $n = 13$ ; serum  $[\text{Cl}^-] = 120$  mM) and regional ASL  $[\text{Cl}^-]$  in rabbit (Trch,  $114.3 \pm 1.8$  mM,  $n = 6$ ; serum  $[\text{Cl}^-] = 105$  mM), bronchus (Brnch;  $126.9 \pm 1.7$  mM,  $n = 3$ ), and small airways (SA;  $108.3 \pm 7.1$  mM,  $n = 5$ ) are shown. Regional ASL  $[\text{Cl}^-]$  in monkey (Brnch,  $112.3 \pm 10.9$  mM,  $n = 3$ ; SA,  $128.5 \pm 6.8$  mM,  $n = 3$ ; serum  $[\text{Cl}^-] = 110$  mM) also is shown. Human nasal liquid  $[\text{Cl}^-]$  after nasal occlusion (Nsl;  $117.3 \pm 11.2$  mM,  $n = 6$ ; plasma  $[\text{Cl}^-] = 104$  mM) is shown for comparison. In all species studied, ASL  $\text{Cl}^-$  values were comparable to the serum/plasma  $[\text{Cl}^-]$ . Serum  $\text{Cl}^-$  values are from Wolford et al. (1986).

to be visually guided into the distal airways to record ASL  $\text{Cl}^-$ -dependent voltages.

#### Evaluation of Ion-selective Electrode Technology

Although  $\text{Cl}^-$ -electrodes offer advantages over the conventional filter paper ASL sampling procedure, several aspects of the measurements need to be considered. For instance, the measurements could be influenced by nonspecific perturbations of the airway surface. However, such alterations in ASL  $[\text{Cl}^-]$  with the small electrode are likely minimal for several reasons. First, with respect to trauma-induced changes in ASL  $[\text{Cl}^-]$ , the catheter electrode is extended at least 1.5-cm into the airways relative to the tip of the bronchoscope. Thus, bronchoscope-induced trauma to the airways is unlikely in the vicinity of the sensor electrode measurement. The electrode itself is fine, and the mouse transepithelial electrical potential measured concurrently with  $\text{Cl}^-$ -electrode measurements was in close agreement with the mouse transepithelial potential reported by others (Takahashi et al., 1993), suggesting electrode-induced trauma was also minimal. Moreover, Ag/AgCl electrodes with diameters up to 16-fold larger than the diameter of the  $\text{Cl}^-$ -sensing electrode have been used to successfully measure the transepithelial potential in the nose (Hofmann et al., 1997; Fajac et al., 1998) and bronchi of humans (Fajac et al., 1998). Second, the interaction of the electrode and ASL was visualized (Fig.

1 B) and local ASL hydrostatic pressure generated by electrode immersion in ASL was calculated. This analysis predicted a negligible change of ASL volume, indicating that the electrode did not significantly affect the ASL ion composition through “wicking” solution along and/or across the airways epithelia (Erjefalt and Persson, 1990; Pilewski and Frizzell, 1999). Taken together, it is unlikely that local trauma or physical forces substantially contributed to the ASL  $\text{Cl}^-$  concentrations reported here with  $\text{Cl}^-$ -electrodes.

Next, because evaporative water loss can artifactually raise ASL  $[\text{Cl}^-]$ , approaches were developed to minimize dehydration of the ASL during our measurements. For human nasal ASL  $[\text{Cl}^-]$  measurements, the nostrils were occluded for  $\geq 10$  min before measurement. For bronchoscopic measurements, the anesthetic was humidified and delivered to rabbits via face mask (rabbits were not intubated). Due to concerns that the anesthetic and gases delivered through an endotracheal tube could not be fully humidified despite the usual humidification maneuvers, only bronchial and small airway  $\text{Cl}^-$  measurements were performed in monkeys. In view of a recent study showing that the ASL osmolality in distal airways was not affected by anesthesia and ventilatory parameters similar to those we used, or even when exposed to dry air (200 ml/min; Freed and Davis, 1999), it is unlikely that the distal ASL  $\text{Cl}^-$  measurements in rabbits and monkeys were significantly affected by anesthetic-induced evaporative  $\text{H}_2\text{O}$  loss.

Next, we evaluated the contribution of the junction potential to our measurements. A 1.1-mV liquid junction potential (reported as the ASL relative to the reference solution) was calculated from the Henderson equation (MacInnes, 1939) together with ASL  $\text{Na}^+$ ,  $\text{K}^+$ , and  $\text{Cl}^-$  concentrations reported from filter paper studies in normal humans (Joris et al., 1993; Knowles et al., 1997) and published ionic mobilities (25°C; Hille, 1992). The junction potential calculated between the reference solution and 30 mM  $\text{Cl}^-$  standard solution was 0.82 mV. A 1-mV uncompensated junction potential contributes an  $\sim 4\%$  error to ASL  $[\text{Cl}^-]$  (Koryta, 1975; Bailey, 1980). Thus, the small decrease in the junction potential between the reference solution and 30 mM  $\text{Cl}^-$  solution during superfusion (Fig. 3) would contribute a negligible error to the  $[\text{Cl}^-]$  reported here.

Because the  $\text{Cl}^-$ -electrode, like all ion-selective electrodes, detects  $\text{Cl}^-$  activity ( $\alpha_{\text{Cl}^-}$ ) and not concentration, the  $\text{Cl}^-$  activity coefficient ( $\gamma_{\text{Cl}^-}$ ) was held constant by setting the calibration solution ionic strength to 150 mM (i.e., the approximately normal human plasma ionic strength) so that the electrode response was proportional to the  $\log[\text{Cl}^-]$  term in Eq. 1. However, this ionic strength is  $\sim 50$  mM larger than the ASL value calculated from the  $\text{Na}^+$ ,  $\text{K}^+$ , and  $\text{Cl}^-$  concentrations previously reported in filter paper studies (Joris et al.,

1993; Knowles et al., 1997). The  $\text{Cl}^-$  error calculated from the change in  $\gamma_{\text{Cl}}$  due to calibrating an electrode in 200 mM ionic strength solutions and sampling from a 100-mM ionic strength test solution was 5.5% (25°C).

Collectively, the combined  $\text{Cl}^-$  error estimated from the junction potential and difference in  $\gamma_{\text{Cl}}$  is comparable to the error associated with  $\text{Cl}^-$  measurements in physiologic salt solutions (within 7%) and the measured error reported with ion-selective electrode measurements in solutions of various ionic strengths ( $\sim 2\%$ , versus standard calomel reference electrode, 37°C; Mohan and Bates, 1975). The measurement error is well within the resolution necessary to distinguish between current controversial hypotheses regarding the ASL  $[\text{Cl}^-]$  (i.e.,  $\text{Cl}^- \leq 50$  mM or  $\geq 100$  mM; Widdicombe, 1999; Wine, 1999).

#### *In Vivo ASL $[\text{Cl}^-]$ Measurements of Human Nasal Liquid: Basal and with Evaporative $\text{H}_2\text{O}$ Loss*

The ASL  $[\text{Cl}^-]$  value recorded (117 mM) from the fully humidified nasal surface (i.e., postnasal occlusion) is similar to other studies that used filter papers to collect nasal liquid after that maneuver (Knowles et al., 1997; Hull et al., 1998). Specifically, the electrode measurements of nasal  $\text{Cl}^-$  in normal adult humans were 7% lower than the value previously reported from our laboratory under similar conditions (Knowles et al., 1997), and 2% higher than the value reported for normal infants (Hull et al., 1998). Taken together, these data strongly suggest that normal nasal ASL  $[\text{Cl}^-]$  exceeds 100 mM in the basal (fully humidified) state.

The highest  $[\text{Cl}^-]$  ( $\sim 150$  mM) was measured in the nasal liquid collected during nasal breathing, i.e., before occlusion. Based on previous studies, the elevated  $[\text{Cl}^-]$  was likely due to evaporative  $\text{H}_2\text{O}$  loss from the nasal surface liquid residing in the poorly humidified environment of the proximal turbinates. For example, evaporative  $\text{H}_2\text{O}$  loss from the surface of proximal airways during inspiration of dry air has been shown to increase the ASL osmolality (Jayaraman et al., 2001b) and  $[\text{Cl}^-]$  (Man et al., 1979; Boucher et al., 1981a).

#### *Large Airway (Tracheobronchial) ASL $[\text{Cl}^-]$*

The  $\text{Cl}^-$  concentrations reported here for the rabbit trachea and rabbit and monkey bronchi exceed 100 mM (range: 112–127 mM) and are similar to the  $\text{Cl}^-$  values reported in excised human bronchi with fluorescence measurements (92 mM; Jayaraman et al., 2001a). The  $\text{Cl}^-$  values reported in human (84–88 mM; Joris et al., 1993; Knowles et al., 1997) and sheep (91 mM; Mentz et al., 1986) that were obtained from samples of ASL collected with filter paper in vivo are somewhat lower than the electrode data. Filter paper-induced submucosal gland secretion of hypotonic fluid into the airways was suggested to lower the ASL ion composi-

tion in human bronchi (Knowles et al., 1997). Rabbits have few if any submucosal glands (Choi et al., 2000; Harkema et al., 1991; Jarnigan et al., 1983) and these glands are less abundant in monkeys compared with humans (Goco et al., 1963). Thus, the relatively higher monkey and rabbit bronchus ASL  $\text{Cl}^-$  values could result from minimal to no submucosal gland secretion at the site of the electrode recording in these species.

#### *Mouse Tracheal ASL $[\text{Cl}^-]$*

The mouse tracheal  $\text{Cl}^-$  was in excess of 100 mM and is comparable ( $\sim 20\%$  lower) to the mouse tracheal  $\text{Cl}^-$  value recently reported using a novel in vivo fluorescence detection strategy (Jayaraman et al., 2001a). Whereas Jayaraman et al. (2001a) used atropine to inhibit submucosal gland secretion in some experiments, we did not use atropine and, therefore, cannot rule out a contribution of (hypotonic) gland secretion in our  $\text{Cl}^-$  measurements. Alternatively, because respiration was not interrupted during Jayaraman et al.'s (2001a) study, their measurements are likely to more closely reflect the mouse tracheal ASL  $\text{Cl}^-$  during respiration.

However, compared with other studies, our tracheal  $\text{Cl}^-$  values are well above the  $\text{Cl}^-$  concentrations reported in vivo in mouse ( $\sim 57$  mM) using a microcapillary collection technique (Cowley et al., 2000) or in mouse tracheal cultures ( $\sim 10$  mM; McCray et al., 1999). Condensation of humidified air within the microcapillary glass during collection could have contributed to low  $[\text{Cl}^-]$  reported with the in vivo microcapillary technique. Difficulties in achieving the rapid sampling of ASL required when making measurements of ASL  $\text{Cl}^-$  concentrations using tritiated water and  $^{36}\text{Cl}^-$  may have accounted for the low values in vitro. We would note that the simultaneous measurements of transepithelial electrical potential difference with the  $\text{Cl}^-$ -electrode measurements would appear to control for trauma-induced artifacts in mouse ASL  $[\text{Cl}^-]$  reported here.

#### *Rabbit and Monkey Small Airway (Bronchiolar) ASL $[\text{Cl}^-]$*

Knowledge of the ASL  $[\text{Cl}^-]$  in the small diameter airways (i.e., bronchioles) is important because of the relevance to early CF lung disease (Davis et al., 1996). However, due to the relative inaccessibility to this region in vivo, little is known of the small diameter airways ASL ion composition. Both rabbit and monkey small airways exhibited an ASL  $[\text{Cl}^-] > 100$  mM ( $108 \pm 7$  mM,  $n = 5$ ; and  $129 \pm 7$  mM,  $n = 53$ , respectively).

Monkey small airways ASL  $[\text{Cl}^-]$  was  $\sim 15\%$  higher than bronchus and was larger than in any other region of all species studied under similar (i.e., humidified) conditions. Interestingly, compared with monkey, the regional ASL  $\text{Cl}^-$  differences in rabbit were essentially reversed. Rabbit small airways exhibited the lowest ASL  $[\text{Cl}^-]$  (but similar to the monkey bronchus  $\text{Cl}^-$  value),

being ~18% lower than in bronchus. Differences in ASL  $[Cl^-]$  between large and small airways in rabbits and monkeys may reflect species-specific regional differences in the regulation of other ASL anions, e.g.,  $HCO_3^-$ . These results suggest that normal bronchioles produce a “high” rather than low ionic strength ASL, which is consistent with the isotonic model of ASL physiology. “Isotonic” physiology is congruent with other measures of the physiology of this region, such as the low transepithelial resistance in excised pig small airways (Inglis et al., 1996) and the high epithelial osmotic water permeability coefficients in guinea pig small airways (Folkesson et al., 1996).

### Summary

A key prediction of the compositional hypothesis is that normal ASL  $[Cl^-]$  is maintained at  $\leq 50$  mM to permit defensins to be active in bacterial killing (Smith et al., 1996). Conversely, defensins are predicted to be inactive in  $[Cl^-] \geq 100$  mM that is presumed to be a unique feature of CF ASL (Goldman et al., 1997). However, our results strongly suggest that in both the normal human nasal cavity and in large and small airways of three different mammalian species, the ASL  $[Cl^-]$  normally exceeds 100 mM (Fig. 6). These findings suggest that it is very unlikely that normal lung defense is mediated by low ASL  $[Cl^-]$ /defensin activity. Whereas we have not measured all solution ions to estimate ASL tonicity, the ASL  $[Cl^-]$  is in the range of plasma  $[Cl^-]$ . Based on these data, and previous reports of others of direct measurements of ASL osmolality in vivo (Boucher et al., 1981b; Verkman, 2001), it appears more likely that airways defense is mediated by isotonic volume transport and mucus clearance (Matsui et al., 1998; Tarran et al., 2001b).

We gratefully acknowledge D.J. Gillie, C. Campbell, W.T. Harris, M.D., and K.W. Southern, M.D., Ph.D., for technical assistance.

This work was supported by grants from the National Institutes of Health (RR00046 [to M.R. Knowles] and HL60280 [to R.C. Boucher]) and the Cystic Fibrosis Foundation (RO26 [to R.C. Boucher]).

Submitted: 15 October 2001

Revised: 6 November 2001

Accepted: 8 November 2001

### REFERENCES

- Bacconnais, S., J. Zahm, L. Kilian, P. Bonhomme, D. Gobillard, A. Perchet, E. Puchelle, and G. Balossier. 1998. X-ray microanalysis of native airway surface liquid collected by cryotechnique. *J. Microsc.* 191:311–319.
- Bailey, P.L. 1980. Analysis with Ion-Selective Electrodes. 2nd. ed. Heyden, Philadelphia. 247 pp.
- Bals, R., X. Wang, Z. Wu, T. Freeman, V. Bafna, M. Zasloff, and J.M. Wilson. 1998. Human beta-defensin 2 is a salt-sensitive peptide antibiotic expressed in human lung. *J. Clin. Invest.* 102:874–880.
- Bals, R., D.J. Weiner, and J.M. Wilson. 1999. The innate immune system in cystic fibrosis lung disease. *J. Clin. Invest.* 103:303–307.
- Boucher, R.C., M.J. Stutts, P.A. Bromberg, and J.T. Gatzky. 1981a. Regional differences in airway surface liquid composition. *J. Appl. Physiol.* 50:613–620.
- Boucher, R.C., M.J. Stutts, and J.T. Gatzky. 1981b. Regional differences in bioelectric properties and ion flow in excised canine airways. *J. Appl. Physiol.* 51:706–714.
- Boucher, R.C., M.J. Stutts, M.R. Knowles, L. Cantley, and J.T. Gatzky. 1986.  $Na^+$  transport in cystic fibrosis respiratory epithelia. Abnormal basal rate and response to adenylate cyclase activation. *J. Clin. Invest.* 78:1245–1252.
- Choi, H.K., W.E. Finkbeiner, and J.H. Widdicombe. 2000. A comparative study of mammalian tracheal mucous glands. *J. Anat.* 197:361–372.
- Cowley, E.A., K. Govindaraju, C. Guilbault, D. Radzioch, and D.H. Eidelman. 2000. Airway surface liquid composition in mice. *Am. J. Physiol.* 278:L1213–L1220.
- Davis, P.B., M. Drumm, and M.W. Konstan. 1996. Cystic fibrosis. *Am. J. Respir. Crit. Care Med.* 154:1229–1256.
- Durand, J., W. Durand-Arczynska, and P. Haab. 1981. Volume flow, hydraulic conductivity and electrical properties across bovine tracheal epithelium in vitro: effect of histamine. *Pflügers Arch.* 392:40–45.
- Erjefelt, I., and C.G. Persson. 1990. On the use of absorbing discs to sample mucosal surface liquids. *Clin. Exp. Allergy.* 20:193–197.
- Fajac, I., J. Lacroinque, A. Lockhart, J. Dall’Ava-Santucci, and D.J. Dusser. 1998. Silver/silver chloride electrodes for measurement of potential difference in human bronchi. *Thorax.* 53:879–881.
- Folkesson, H.G., M.A. Matthay, A. Frigeri, and A.S. Verkman. 1996. Transepithelial water permeability in microperfused distal airways. Evidence for channel-mediated water transport. *J. Clin. Invest.* 97:664–671.
- Freed, A.N., and M.S. Davis. 1999. Hyperventilation with dry air increases airway surface fluid osmolality in canine peripheral airways. *Am. J. Respir. Crit. Care Med.* 159:1101–1107.
- Goco, R.V., M.B. Kress, and O.C. Brantigan. 1963. Comparison of mucus glands in the tracheal bronchial tree of man and animals. *Ann. NY Acad. Sci.* 106:555–571.
- Goldman, M.J., G.M. Anderson, E.D. Stolzenberg, U.P. Kari, M. Zasloff, and J.M. Wilson. 1997. Human beta-defensin-1 is a salt-sensitive antibiotic that is inactivated in cystic fibrosis. *Cell.* 88:553–560.
- Hansen, L., M. Buechele, J. Koroshec, and W.J. Warwick. 1968. Sweat chloride analysis by chloride ion-specific electrode method using heat stimulation. *Am. J. Clin. Pathol.* 49:834–841.
- Harkema, J.R., A. Mariassy, J. St. George, D.M. Hyde, and C.G. Plopper. 1991. Epithelial cells of the conducting airways: a species comparison. *In The Airway Epithelium. Physiology, Pathophysiology, and Pharmacology.* S.G. Farmer and D.W.P. Hay, editors. Marcel Dekker, New York. 3–39.
- Hille, B. 1992. Elementary properties of ions in solutions. *In Ionic Channels of Excitable Membranes.* Sinauer Associates, Inc., Sunderland, MA. 261–290.
- Hofmann, T., O. Boehmer, P. Bittner, G. Huels, H.G. Terbrack, E. Heerd, and H. Lindemann. 1997. Conventional and modified nasal potential difference measurement: clinical use in cystic fibrosis. *Am. J. Respir. Crit. Care Med.* 155:1908–1913.
- Hull, J., W. Skinner, C. Robertson, and P. Phelan. 1998. Elemental content of airway surface liquid from infants with cystic fibrosis. *Am. J. Respir. Crit. Care Med.* 157:10–14.
- Inglis, S.K., M.R. Corboz, A.E. Taylor, and S.T. Ballard. 1996. Regulation of ion transport across porcine distal bronchi. *Am. J. Physiol.* 270:L289–L297.
- Jarnigan, F., J.D. Davis, P.A. Bromberg, J.T. Gatzky, and R.C. Boucher. 1983. Bioelectric properties and ion transport of excised rabbit trachea. *J. Appl. Physiol.* 55:1884–1892.
- Jayaraman, S., Y. Song, L. Vetrivel, L. Shankar, and A.S. Verkman. 2001a. Noninvasive in vivo fluorescence measurement of airway-

- surface liquid depth, salt concentration, and pH. *J. Clin. Invest.* 107:317–324.
- Jayaraman, S., Y. Song, and A.S. Verkman. 2001b. Airway surface liquid osmolality measured using fluorophore-encapsulated liposomes. *J. Gen. Physiol.* 117:423–430.
- Joris, L., I. Dab, and P.M. Quinton. 1993. Elemental composition of human airway surface liquid in healthy and diseased airways. *Am. Rev. Respir. Dis.* 148:1633–1637.
- Knowles, M.R., J.M. Robinson, R.E. Wood, C.A. Pue, W.M. Mentz, G.C. Wager, J.T. Gatzky, and R.C. Boucher. 1997. Ion composition of airway surface liquid of patients with cystic fibrosis as compared to normal and disease-control subjects. *J. Clin. Invest.* 100:2588–2595.
- Kopito, L., and H. Shwachman. 1969. Studies in cystic fibrosis: determination of sweat electrolytes in situ with direct reading electrodes. *Pediatrics.* 43:794–798.
- Koryta, J. 1975. *Ion-Selective Electrodes.* Cambridge University Press, New York. 207 pp.
- Krouse, M.E. 2001. Is cystic fibrosis lung disease caused by abnormal ion composition or abnormal volume? *J. Gen. Physiol.* 118:219–222.
- Landry, J.S., K. Govindaraju, C. Landry, and D.H. Eidelman. 2000. The use of polyethylene catheters to harvest ASL: role of surface tension. *Pediatr. Pulmonol. Suppl.* 20:271A. (Abstr.)
- MacInnes, D.A. 1939. Galvanic cells with liquid junction potentials. *In* The Principles of Electrochemistry. Reinhold, New York. 220–245.
- Man, S.F.P., G.K. Adams, III, and D.F. Proctor. 1979. Effects of temperature, relative humidity, and mode of breathing on canine airway secretions. *J. Appl. Physiol.* 46:205–210.
- Matsui, H., B.R. Grubb, R. Tarran, S.H. Randell, J.T. Gatzky, C.W. Davis, and R.C. Boucher. 1998. Evidence for periciliary liquid layer depletion, not abnormal ion composition, in the pathogenesis of cystic fibrosis airways disease. *Cell.* 95:1005–1015.
- McCray, P.B., Jr., J. Zabner, H.P. Jia, M.J. Welsh, and P.S. Thorne. 1999. Efficient killing of inhaled bacteria in deltaF508 mice: role of airway surface liquid composition. *Am. J. Physiol.* 277:L183–L190.
- Mentz, W.M., J.B. Brown, M. Friedman, M.J. Stutts, J.T. Gatzky, and R.C. Boucher. 1986. Deposition, clearance, and effects of aerosolized amiloride in sheep airways. *Am. Rev. Respir. Dis.* 134:938–943.
- Mohan, M.S., and R.G. Bates. 1975. Calibration of ion-selective electrodes for use in biological fluids. *Clin. Chem.* 21:864–872.
- Pilewski, J.M., and R.A. Frizzell. 1999. Role of CFTR in airway disease. *Physiol. Rev.* 79(Suppl):S215–S255.
- Schwiebert, E.M., D.J. Benos, M.E. Egan, M.J. Stutts, and W.B. Guggino. 1999. CFTR is a conductance regulator as well as a chloride channel. *Physiol. Rev.* 79(Suppl):S145–S166.
- Sheppard, D.N., and M.J. Welsh. 1999. Structure and function of the CFTR chloride channel. *Physiol. Rev.* 79(Suppl):S23–S45.
- Smith, J.J., S.M. Travis, E.P. Greenberg, and M.J. Welsh. 1996. Cystic fibrosis airway epithelia fail to kill bacteria because of abnormal airway surface fluid. *Cell.* 85:229–236.
- Stutts, M.J., C.M. Canessa, J.C. Olsen, M. Hamrick, J.A. Cohn, B.C. Rossier, and R.C. Boucher. 1995. CFTR as a cAMP-dependent regulator of sodium channels. *Science.* 269:847–850.
- Takahashi, M., S.R. Kleeberger, and T.L. Croxton. 1993. Effects of ozone on transepithelial potential of mouse trachea. *Am. J. Physiol.* 265:L33–L37.
- Tarran, R., and R.C. Boucher. 2001. Thin-film measurements of airway surface liquid volume/composition and mucus transport rates in vitro. *In* Cystic Fibrosis Methods and Protocols. W.R. Skach, editor. Humana Press, Totowa, NJ. 479–492.
- Tarran, R., B.R. Grubb, J.T. Gatzky, C.W. Davis, and R.C. Boucher. 2001a. The relative roles of passive surface forces and active ion transport in the modulation of airway surface liquid volume and composition. *J. Gen. Physiol.* 118:223–236.
- Tarran, R., B.R. Grubb, D. Parsons, M. Picher, A.J. Hirsch, C.W. Davis, and R.C. Boucher. 2001b. The CF salt controversy: In vivo observations and therapeutic approaches. *Mol. Cell.* 8:149–158.
- Travis, S.M., B.A. Conway, J. Zabner, J.J. Smith, N.N. Anderson, P.K. Singh, E.P. Greenberg, and M.J. Welsh. 1999. Activity of abundant antimicrobials of the human airway. *Am. J. Respir. Cell Mol. Biol.* 20:872–879.
- Verkman, A.S. 2001. Lung disease in cystic fibrosis: is airway surface liquid composition abnormal? *Am. J. Physiol. Lung Cell Mol. Physiol.* 281:L306–L308.
- Widdicombe, J.H. 1999. Altered NaCl concentration of airway surface liquid in cystic fibrosis. *News Physiol. Sci.* 14:126–127.
- Wine, J.J. 1999. The genesis of cystic fibrosis lung disease. *J. Clin. Invest.* 103:309–312.
- Wolford, S.T., R.A. Schroer, F.X. Gohs, P.P. Gallo, M. Brodeck, H.B. Falk, and R. Ruhren. 1986. Reference range data base for serum chemistry and hematology values in laboratory animals. *J. Toxicol. Environ. Health.* 18:161–188.